applied sciences

MDPI

Article

Analysis of Shear Constitutive Models of the Slip Zone Soil Based on Various Statistical Damage Distributions

Yinfeng Luo [1], Zongxing Zou [1,*], Changdong Li [2], Haojie Duan [1], Nang Mon Mon Thaw [2], Bocheng Zhang [2], Bingdong Ding [2] and Junrong Zhang [2]

[1] Badong National Observation and Research Station of Geohazards, China University of Geosciences, Wuhan 430074, China; luoyinfeng@cug.edu.cn (Y.L.); duanhaojie184@foxmail.com (H.D.)
[2] School of Engineering, China University of Geosciences, Wuhan 430074, China; lichangdong@cug.edu.cn (C.L.); nanmonmonthaw.geol@tgu.edu.mm (N.M.M.T.); zhangbocheng@cug.edu.cn (B.Z.); dingbd@cug.edu.cn (B.D.); zjr@cug.edu.cn (J.Z.)
* Correspondence: zouzongxing@cug.edu.cn

Abstract: The shear constitutive model of the slip zone soil can be used to quantitatively describe the relationship between shear stress and shear displacement, which is of great significance for the analysis of deformation mechanism and stability evaluation of landslides. The conventional shear constitutive models were usually proposed based on statistical damage theory with the Weibull distribution function, which is widely used in the field of rock material. However, there are great differences in the structure and mechanical properties of soil and rock; therefore, the suitability of the damage distribution functions for the slip zone soil needs to be further investigated. In this study, eight distribution functions are introduced to describe the damage evolution process of the slip zone soil and applied to two groups of shear stress–shear displacement curves (named shear curves) with different softening characteristics, i.e., strong softening type and weak softening type. The results show that: (1) the applicability of the various damage distribution functions to the two softening types of shear curves is obviously different; (2) the commonly used Weibull distribution is only suitable for the weak softening shear curves; (3) the shear constitutive models based on Gamma, Exponential, and Logistic distributions are the best three models for the strong softening curve; the shear constitutive models based on Gamma, Weibull, and Exponential distributions are the best three models for the weak softening curve; (4) Gamma distribution function is the optimal model in both strong softening and weak softening types of shear curves, and the parameters of the function have clear physical meaning in the shear constitutive model. In general, the Gamma distribution function can more objectively reflect the whole shear damage evolution process of the slip zone soil than other distribution functions.

Keywords: landslide; statistical damage; strain softening; sliding zone soil; ring shear test

Citation: Luo, Y.; Zou, Z.; Li, C.; Duan, H.; Thaw, N.M.M.; Zhang, B.; Ding, B.; Zhang, J. Analysis of Shear Constitutive Models of the Slip Zone Soil Based on Various Statistical Damage Distributions. *Appl. Sci.* **2022**, *12*, 3493. https://doi.org/10.3390/app12073493

Academic Editors: Qingbing Liu and Youkou Dong

Received: 2 March 2022
Accepted: 26 March 2022
Published: 30 March 2022

1. Introduction

The failure of a landslide is mostly controlled by the weak unit inside the landslide, which is usually called the slip zone. The evolution process of landslides is accompanied by the shear deformation of slip zone soil and progressive deterioration of mechanical strength [1–5]. The strength of slip zone soil decreases from peak strength to residual strength with the deformation of slip zone soil, which is a very common process, named strain softening phenomenon [4]. The constitutive model of soil is a formula reflecting the relationship between stress and deformation of soil mass. Therefore, constructing a constitutive model that can describe the strain softening property is of great significance to investigate the mechanical behavior of landslides [6–8].

Many constitutive models representing strain softening of rock and soil have been established through experimental and theoretical research. Before the peak of stress–strain

curves, the hyperbolic model and piecewise linear model were proposed [9–11]; after the peak of stress–strain curves, strength abruptly falling model [12,13], linear attenuation model, and hyperbolic attenuation model was proposed [14,15]. However, these models only reflect the relationship between stress and strain and cannot intuitively represent the characteristics of large deformation of slip zone soil. Recently, a shear constitutive model describing the relationship between shear stress and shear displacement is proposed based on statistical damage mechanics [16–18]. It has obvious advantages of representing the large deformation mechanics of slip zone soil and providing the basis for dynamic evaluation of landslide stability.

Statistical damage mechanics have been widely used in the constitutive models of rock materials [19–24]. In recent years, the statistical damage mechanics of rock have been introduced into the soil field [16–18,25,26]. Based on statistical damage, the damage variable can be defined as the damage degree of the material. The distribution of damage variables (damage distribution) with displacement in the shear constitutive model represents the damage evolution with shear displacement. However, the damage distribution of soil directly adopts the Weibull distribution function [27], which is widely used in the rock damage mechanical field. In fact, due to the great differences between structural and mechanical properties of soil and rock, the damage distribution function of soil may differ from that of rock. Therefore, the damage distribution function of the slip zone soil needs to be further investigated.

A large number of ring shear test results of slip zone soil show that the shear stress–shear displacement curves (named shear curves) can be classified into two types including weak softening curve and strong softening curve. The weak softening type curve (Figure 1a) has a low softening degree and a small difference between the peak strength and the residual strength; in contrast, the strong softening curve (Figure 1b) has a high softening degree and a large difference between the peak strength and the residual strength. By searching the keyword 'ring shear' from 2000 to 2020 in the web of science database, 32 valid papers about ring shear tests were retrieved, presenting 104 groups of soil ring shear test data. Among them, 54 groups belong to the weak softening curve, accounting for 52%; 50 groups belong to the strong softening curve, accounting for 48%. The curves of different softening types reflect the different damage evolution characteristics in the process of soil shear, which may affect the applicability of the selected damage distribution function. Therefore, more distribution functions are needed to verify the damage distribution model suitable for different slip zone soil curves.

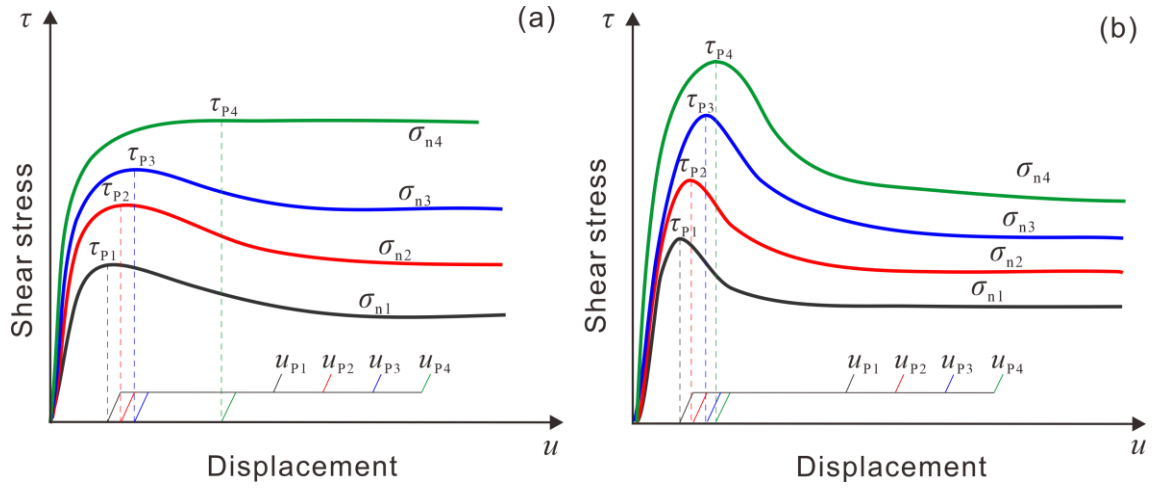

Figure 1. Two kinds of softening characteristic shear stress–shear displacement curves. (**a**) Weak softening curve; (**b**) strong softening curve; normal stress: $\sigma_{n1} < \sigma_{n2} < \sigma_{n3} < \sigma_{n4}$.

Focusing on the selection of damage distribution in constructing the shear constitutive model of slip zone soil, this study investigates the possible damage distribution functions for describing the damage evolution process of the soil. The fitting method is adopted instead of the previous method of solving model parameters through peak value. This method can better show the fitting effect of the constitutive model on the shear curve, especially in the strain softening stage. Then, the applicability of various distribution functions for two groups of shear curves in slip zone soil were analyzed with different softening degrees. Finally, the optimal damage distribution suitable for different softening types of curves was determined.

2. Shear Constitutive Models of Slip Zone Soil

The strain softening phenomenon often occurs in the process of large shear deformation of landslides; that is, the shear stress decreases with displacement when the shear stress exceeds the peak. According to a large number of ring shear test results, the whole process of shear deformation and failure of slip zone soil can be divided into five stages (Figure 2): the pore compaction stage (Stage 1 in Figure 2); the elastic deformation stage (Stage 2 in Figure 2); the plastic hardening stage (Stage 3 in Figure 2); the strain softening stage (Stage 4 in Figure 2); and the residual strength stage (Stage 5 in Figure 2). The shear characteristics of the above stages should be taken into consideration in the establishment of the shear constitutive model of slip zone soil.

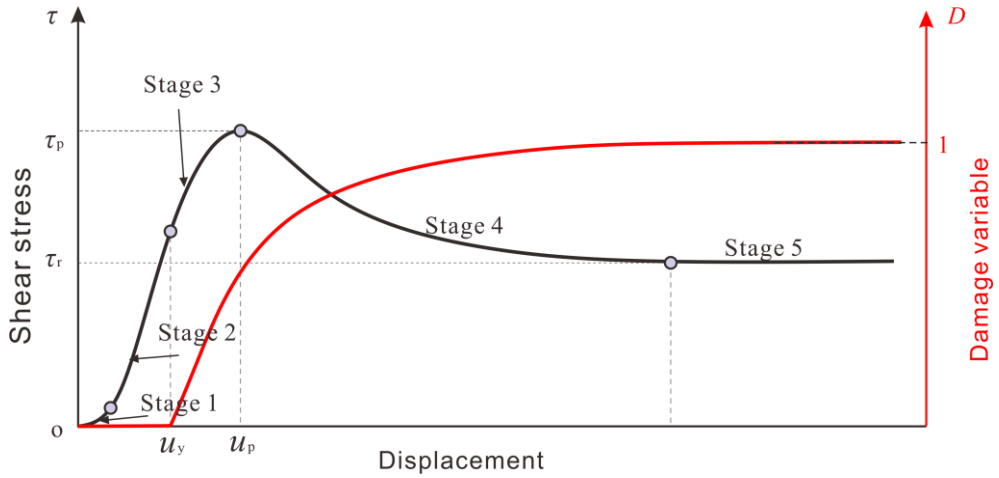

Figure 2. Shear stress–shear displacement curve and damage evolution curve of the slip zone soil in the whole shear process. The damage variable D can define the damage degree of the soil. The damage variable of 0 indicates that the soil is not damaged, and the damage variable of 1 indicates that the soil is completely damaged.

During the shearing process of the slip zone, the slip zone soil is progressively damaged. In this process, the shear stress of soil is jointly undertaken by the damaged part and the intact part. According to the strain equivalent hypothesis [21], the strength relationship of the microelement of the slip zone soil based on the statistical damage can be obtained:

$$\tau = \tau'(1 - D) + \tau'' D \quad (1)$$

where τ'' is the shear stress of the damaged part, τ' is the shear stress of the intact part and τ is the total shear stress of the soil; D is the damage variable of soil, which changes with the process of shear failure and deformation.

There are many methods to define the damage variable D. In the shear process of slip zone soil, the damage variable D can be defined as the ratio of the damaged part area and the total area of the shear body (Figure 3):

$$D = \frac{N_D}{N} \tag{2}$$

where N_D is the area of damage microelement and N is the total area of microelement soil. When the soil is not damaged, the damage element N_D is 0, and the damage variable D is 0. When the soil is completely destroyed, the intact elements are totally transformed into the damaged elements, and the damage variable D is 1, as shown in Figure 2.

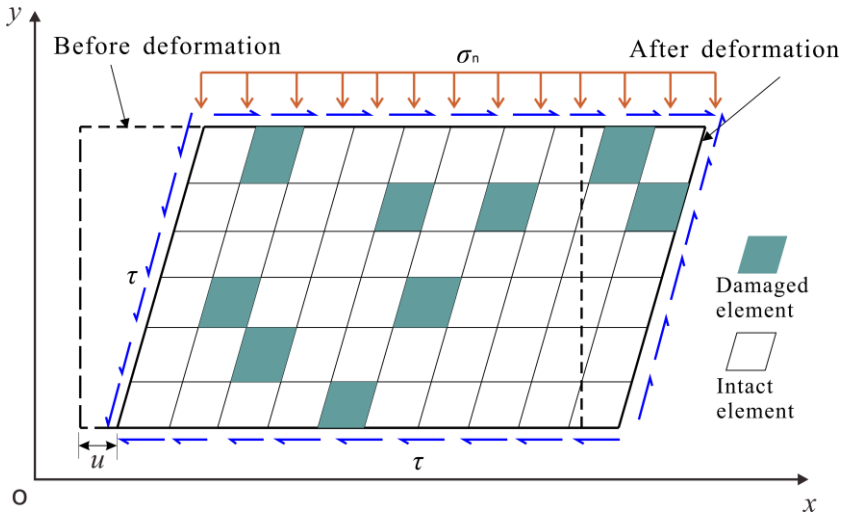

Figure 3. Damage model of soil microelement in shear process of slip zone soil.

The soil microelements can be divided into two parts: intact element and damaged element, as shown in Figure 3. According to the mechanical response model of soil microelement (Figure 4), the soil element is an elastic component with shear stiffness K_s in the stage without damage, which maintains elastic deformation and follows Hooke's law, i.e., $\tau' = K_s u$. When the displacement of the element exceeds the critical displacement u_y in the shear process, a part of the intact element is transformed into the damaged element, which obeys a certain random distribution in the soil. Because the strength of the soil decreases to the residual strength when it is completely damaged, the shear stress of the damaged element is equal to the residual strength, i.e., $\tau'' = \tau_r$. Therefore, the strength of the soil is provided by both the intact parts and damaged parts and can be expressed as:

$$\tau = K_s u(1 - D) + \tau_r D \tag{3}$$

where K_s is the slope of the linear elastic stage of the shear curve; τ_r is the residual strength; K_s and τ_r can be obtained from shear test data; u is the shear displacement.

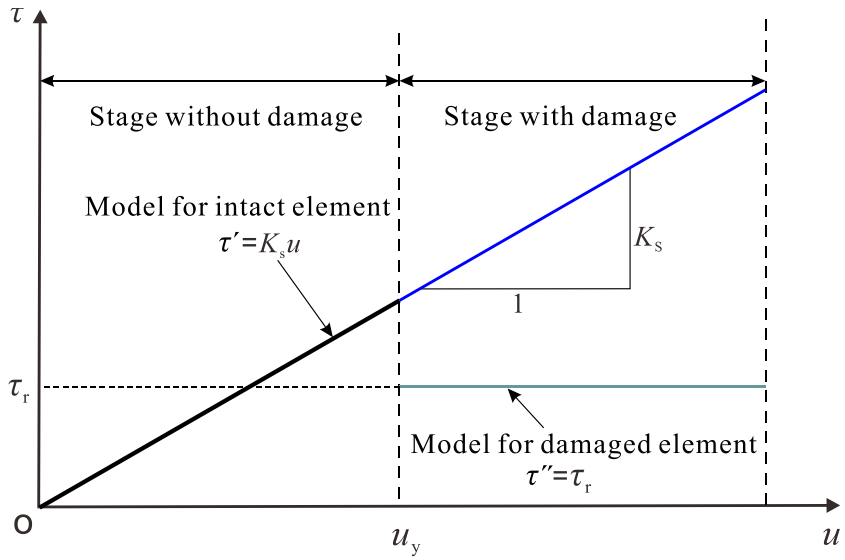

Figure 4. Mechanical response model of soil microelement.

According to the statistical damage, the microelement strength level of the material obeys certain random distribution characteristics (Figure 3). The Weibull function is often used to describe the distribution characteristics of microelement strength in rock and soil [16,22,28,29]. The distribution characteristics of microelement strength reflect the risk probability of failure of slip zone soil, and the failure strength is determined by the strength criterion. In the process of shear deformation, the microelement strength level of slip zone soil changes with shear displacement, which can be expressed by the probability density function $P(u)$ with shear displacement u. The microelement strength level represents the distribution of failure strength under different displacements. The damage distribution representing damage variable D under different displacements can be obtained by integrating the microelements strength level.

$$D(u) = \int_0^u P(u)\mathrm{d}u \tag{4}$$

Equation (4) demonstrates the dynamic process of soil damage evolution in the process of shear deformation. As the soil deforms to failure, the damage variable D increases gradually from 0 to 1.

Substituting Equation (4) into Equation (3) yields

$$D(u) = \int_0^u P(u)\mathrm{d}u \tag{5}$$

Equation (5) shows that the shear constitutive model is dependently related to the microelement strength distribution (or the damage distribution). Selection of the microelement strength distribution function (or the damage distribution function) and determining the parameters of the function are critical for constructing the shear constitutive model.

3. Various Damage Distribution Functions and Solution of Critical Parameters

To describe the distribution law of damage variable in the shear process of slip zone soil, eight kinds of commonly used cumulative distribution functions (CDF) are introduced in this study (Figure 5). These statistical mathematical formulas reflect the microscale and uncertain events in nature and are widely used in various disciplines. This chapter will briefly introduce the commonly used cumulative distribution functions (CDF) to represent the damage distribution in slip zone soil, and the corresponding probability density functions (PDF) represent the microelement strength distribution of soil. Then,

the fitting method is used to solve the function parameters and model curves to judge the distribution function most suitable for different types of shear curves.

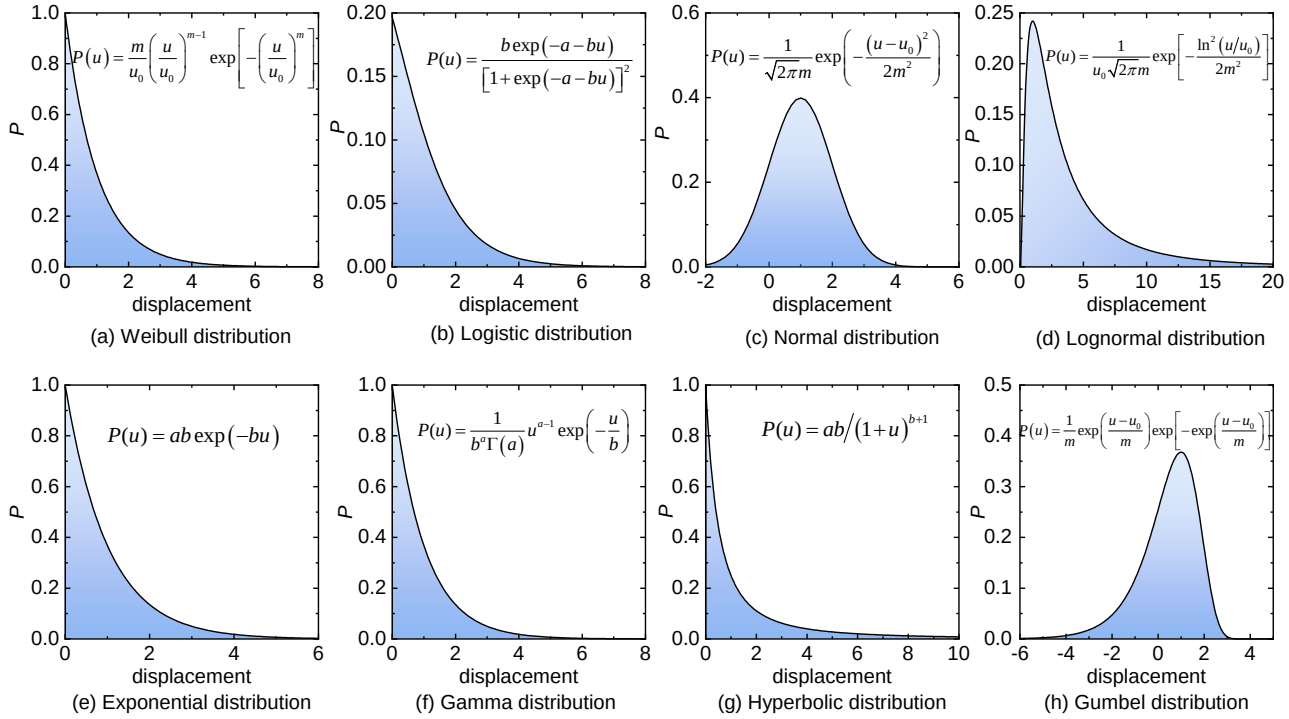

Figure 5. Microelement strength distributions of the soil material are obtained when both parameters of the statistical functions are 1. The black curve represents microelement strength distribution; the blue shaded area represents the damage variable.

3.1. Various Damage Distribution Functions

From the perspective of statistical damage, the damage variable of slip zone soil obeys probability distribution and is a nonlinear function of distribution variable shear displacement (u). Before the yield point displacement u_y, slip zone soil is in the stage of elastic deformation. With the increase of displacement, the shear stress increases linearly. This stage can be regarded as the soil is not damaged; thus the damage variable before the yield point (Figure 2) can be formulated as follows:

$$D = 0 \ (u < u_y) \tag{6}$$

When the shear displacement passes through the displacement at the yield point ($u \geq u_y$), the soil begins to appear with damage deformation (Figure 2). The strength distribution after the yield point can be defined by various PDFs (black curve in Figure 5). Their cumulative distribution functions (blue shaded area in Figure 5) can represent the damage variable.

3.1.1. Weibull Distribution

The Weibull distribution function has been widely used to describe the damage variable of rock [24,29]. The Weibull-PDF is defined as follows:

$$P(u) = \frac{m}{u_0}\left(\frac{u-u_y}{u_0}\right)^{m-1}\exp\left[-\left(\frac{u-u_y}{u_0}\right)^{m}\right], (u \geq u_y) \tag{7}$$

where m and u_0 are the parameters of Weibull distribution function, u_y is the displacement of the yield point, and the Weibull-PDF curve is shown in Figure 5a when u_y is 0.

The damage variable based on Weibull-PDF can be obtained by integral of Equation (7) as follows:

$$D = \int_0^u P(u)du = 1 - \exp[-(\frac{u - u_y}{u_0})^m], (u \geq u_y) \quad (8)$$

3.1.2. Logistic Distribution

The logistic function is widely used in landslide prediction [30]. Liu et al. [31] used it to construct the constitutive model of rock strain softening, but there was a lack of application in the constitutive model of soil. Because the microelement strength distribution is random, the Logistic-PDF can be used to describe the distribution of microelements strength in slip zone soil, as follows:

$$P(u) = \frac{b\exp(-a - bu)}{[1 + \exp(-a - bu)]^2} \quad (9)$$

where a and b are the model parameters. The Logistic-PDF is as shown in Figure 5b.

The damage variable based on Logistic-PDF is obtained as follows:

$$D = \int_0^u P(u)du = \frac{1}{1 + \exp[-(a + bu)]} \quad (10)$$

3.1.3. Normal Distribution

Another common PDF describing the microelement strength distribution is the Normal-PDF (as shown in Figure 5c). Cao et al. [32] have begun to use Normal-PDF to define the microelement strength in the constitutive model of rock strain softening, but it is seldom used in the shear constitutive model of soil. The probability of strength distribution based on Normal distribution is shown as follows:

$$P(u) = \frac{1}{\sqrt{2\pi}m}\exp(-\frac{(u - u_0)^2}{2m^2}), (u \geq u_y) \quad (11)$$

where m and u_0 are the parameters of Normal distribution function. By integrating the above Equation (11), the damage variable based on Normal distribution is obtained as follows:

$$D = \int_0^u P(u)du = \frac{1}{\sqrt{2\pi}m}\int_0^u \exp(-\frac{(u - u_0)^2}{2m^2}), (u \geq u_y) \quad (12)$$

3.1.4. Lognormal Distribution

Lognormal distribution belongs to asymmetric distribution, which is applied to the prediction of landslide regional distribution [33]. When the displacement is small, the shear curve of soil reaches the peak value and enters the softening stage; thus, the probability function of the microelement strength in the slip zone soil may also be asymmetric. The strength distribution with displacement changes as follows:

$$P(u) = \frac{1}{u_0\sqrt{2\pi}m}\exp\left[-\frac{\ln^2((u - u_y)/u_0)}{2m^2}\right], (u \geq u_y) \quad (13)$$

where m and u_0 are the parameters of Lognormal-PDF, and the strength distribution is shown in Figure 5d when u_y is 0.

The damage variable based on Lognormal-PDF is calculated by integrating Equation (13) as follows:

$$P(u) = \frac{1}{u_0\sqrt{2\pi}m}\exp\left[-\frac{\ln^2((u - u_y)/u_0)}{2m^2}\right], (u \geq u_y) \quad (14)$$

3.1.5. Exponential Distribution

Exponential distribution is also used in rock damage constitutive and landslide frequency analysis [34] and can be used to describe the damage evolution of slip zone soil. The Exponential-PDF of microelement strength with displacement is as follows:

$$P(u) = ab\exp(-bu) \tag{15}$$

where a and b are the parameters of Exponential distribution, and the strength distribution is shown in Figure 5e.

By integrating Equation (15), the equation of damage variable based on Exponential distribution is obtained:

$$D = 1 - a\exp(-bu) \tag{16}$$

3.1.6. Gamma Distribution

Gamma distribution is a continuous probability function of statistics, which is a very important distribution in probability statistics. Gamma distribution indicates that there are many identical events in a complex system. This function represents the waiting time for random variable X to wait for event α to occur. In the field of rock, some research has been used to analyze the distribution of discontinuities and the distribution of macropores [35,36]. As the soil is a complex system, the randomness of failure of each microelement is the same, the strength distribution of whole soil can be described by Gamma-PDF, and the formula of probability distribution with displacement is as follows:

$$P(u) = \frac{1}{b^a\Gamma(a)}u^{a-1}\exp\left(-\frac{u}{b}\right) \tag{17}$$

where a is the shape parameter and b is the scale parameter, and the strength distribution is shown in Figure 5f. By integrating Equation (17), the damage evolution formula based on Gamma distribution is obtained:

$$D = \int_0^u P(u)du = \frac{1}{b^a\Gamma(a)}\int_0^u u^{a-1}\exp\left(-\frac{u}{b}\right)du \tag{18}$$

3.1.7. Hyperbolic Distribution

Hyperbolic distribution is widely used in the study of sand particle size distribution under external force [37]. It can be used as a damage evolution model to represent the damage process of slip zone soil as the following formula:

$$D = 1 - \frac{a}{(1+u)^b} \tag{19}$$

where a and b are parameters of the Hyperbolic distribution function.

By calculating the derivative of Equation (19) with respect to the shear displacement u, the distribution function of the microelement strength with the displacement can be obtained as follows:

$$P(u) = \frac{\partial D(u)}{\partial u} = \frac{ab}{(1+u)^{b+1}} \tag{20}$$

when a = 1 and b = 1, the strength distribution is shown in Figure 5g.

3.1.8. Gumbel Distribution

In recent years, with the rapid development of neural networks, Gumbel distribution as a common function of neural networks has been widely used in the field of landslide temporal prediction [38]. Due to the randomness and complexity of damage evolution of slip zone soil, Gumbel distribution can be used to describe the probability distribution of

soil damage, and the Gumbel-PDF of microelement strength about shear displacement can be obtained:

$$P(u) = \frac{\partial D(u)}{\partial u} = \frac{ab}{(1+u)^{b+1}} \tag{21}$$

where u_0 and m are the parameters of the strength distribution. Figure 5h shows the Gumbel-PDF when the parameters u_0 and m are both 1.

By integrating Equation (21), the damage variable based on Gumbel distribution is obtained:

$$D = 1 - \exp\left[-\exp\left(\frac{u-u_0}{m}\right)\right] \tag{22}$$

3.2. Solution Method for the Parameters in the Shear Constitutive Models

There are some parameters that need to be obtained in the shear constitutive model based on statistical damage. The shear stiffness (K_s), yield point displacement (u_y), and residual strength (τ_r) can be directly obtained by ring shear test. There are two unknown parameters (such as a and b, m and u_0) in the above damage distribution functions, which can be expressed as an array β (β_1, β_2). These two parameters are the focus of solving the parameters of the constitutive model. In order to more objectively describe the fitting effect of the constitutive model on the shear curve of soil, a fitting method different from the previous method of solving parameters by peak value is adopted. The commonly used solution method is the iterative least square method. It finds the best matching parameter of test data through the minimum sum of squares of residuals. This method is usable and can give good fitting results for a large number of data. The original shear stress vs. shear displacement data can be obtained by the ring shear test of slip zone soil. The iterative least square method is used to fit the shear constitutive model with the original data. The specific fitting process is shown in Figure 6:

(1) Obtain the test parameters K_s, u_y, and τ_r through ring shear test, then substitute them into the shear constitutive model;
(2) As shown in Figure 6A, substitute the above damage distribution into the constitutive model. Set the initial parameter value β^0 and substitute it into the model;
(3) As shown in Figure 6B, use the least square method to fit, determine the parameter array β corresponding to the minimum sum of squares of residuals (S_{min}). For the convenience of calculation, convert this step to solving the partial derivative of the sum of squares of residuals with respect to parameter array β;
(4) As shown in Figure 6C, use the Gauss–Newton method for iterative calculation. Set the iterative vector to $\Delta\beta$, and iterate the parameter array β at the same time;
(5) When the partial derivative of the sum of squared residuals S is less than the threshold ε, the function is considered to be convergent, and the iterative times is k. Determine the parameter values β^k ($\beta_1{}^k$, $\beta_2{}^k$) of the fitted model.

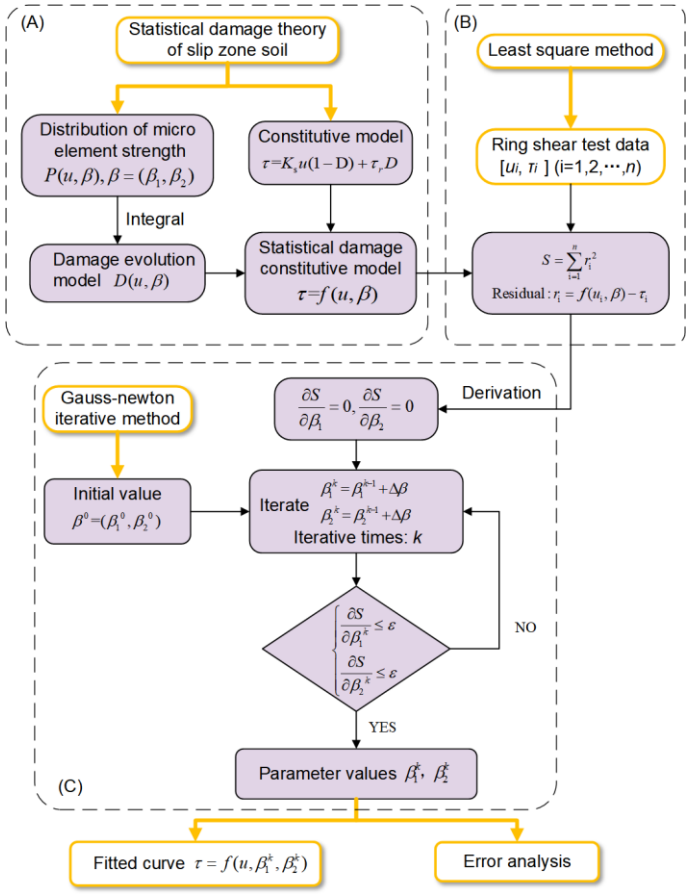

Figure 6. Fitting flow chart of shear constitutive model of slip zone soil. (**A**) Construction of statistical damage constitutive model; (**B**) Least square fitting method; (**C**) Iterative method for solving model parameters.

4. Model Comparison and Validation

4.1. Test Data of Slip Zone Soil

In order to verify the applicability of the constitutive models based on various statistical distributions and analyze the optimal model suitable for different softening types of ring shear curves, the slip zone soils of Huangtupo landslide and Shizibao landslide were selected for experimental comparison [39–41].

The Huangtupo landslide is one of the major landslides in the Three Gorges Reservoir Area (TGRA), located in Badong County (as shown in Figure 7). The Huangtupo landslide is composed of four different slide masses, including the Riverside Slump I#, the Garden Spot Landslide, the Riverside Slump II#, and the Substation Landslide. The slip zone soil samples were taken from test tunnel TP4, which is located in the Riverside Slump II#. The samples were silty clay with gravels in which the content of particles less than 0.075 mm was 40.2%~62.2%, the content of silt was 27.6%~35.5%, with a plasticity index of 7.84%~10.99%. The natural density was 2.09~2.34 g/cm^3, and the natural water content was 12.07%~15.33%.

The Shizibao landslide is located on the south bank of the Yangtze River in Guojiaba Town, Zigui County, TGRA [40,41]. Field investigation shows that this landslide is a rockslide with is bedding plane failure mode. The slip zone soil samples were collected from the slip zone of the Shizibao rockslide, exposed at the left boundary of the landslide site. The samples were of a predominantly sandy texture with 90% of the sand and silt. They have 50% of platy clay minerals that involve illite and montmorillonite, 20% of feldspar and 29% of quartz minerals, with a plasticity index of 13%. The dry density of the samples was 1.77g/cm^3, and the natural water content was 7–8%.

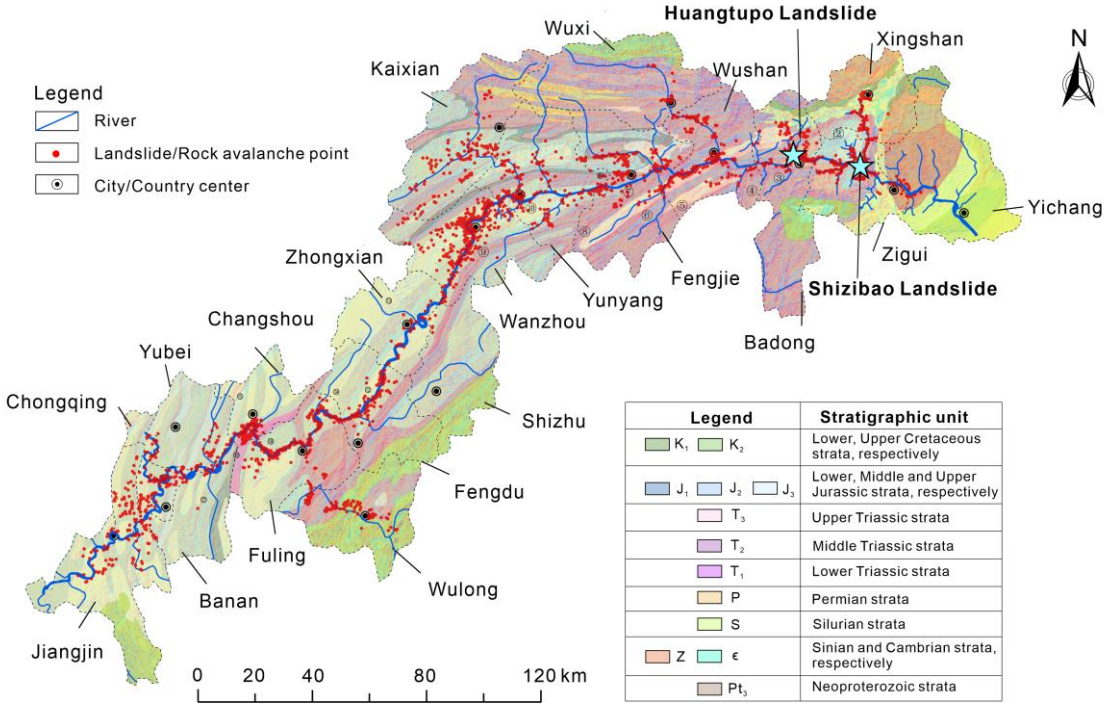

Figure 7. Geological map of TGRA showing the locations of landslides and rock avalanches (Geological map from Tang et al. 2019 [42]).

The ring shear test data of the above two slip zone soil samples represent two types of shear stress–displacement curves with different softening features. The softening characteristic of the slip zone soil of Huangtupo landslide was not obvious and even shows hardening under high normal stress. As shown in Figure 8a, it can represent the shear curve of the weak softening type (Type A curve). The test curve of slip zone soil in the Shizibao landslide has characteristics of large softening degree, as shown in Figure 8b, which can represent the shear curve of strong softening type (Type B curve). These two types of test curves are representative for analyzing the applicability of various constitutive models and softening characteristics of different shear curves.

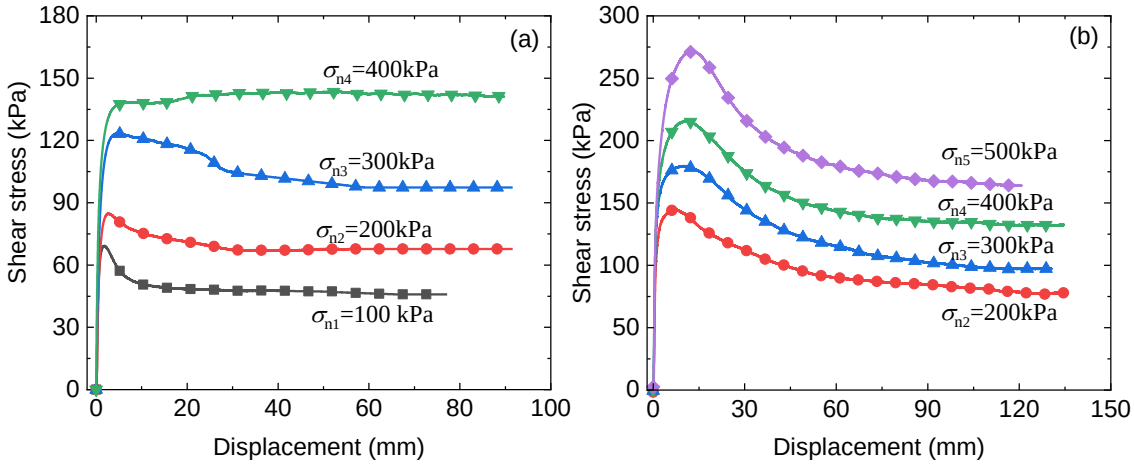

Figure 8. Ring shear test curve of slip zone soil. (**a**) Ring shear test curve of slip zone soil from Huangtupo landslide; (**b**) ring shear test curve of slip zone soil from Shizibao landslide.

4.2. Comparison Results of the Proposed Models

The ring shear test data were fitted by the shear constitutive model with different damage statistical distribution functions. Series A of Figure 9 present the experiment and model result of slip zone soil from the Huangtupo landslide, which represents weak softening shear curves (Type A curves). In contrast, series B of Figure 10 presents the experiment and model result of slip zone soil from the Shizibao landslide, which represents the strong softening shear curves (Type B curves). The values of 1~8, as shown in Figures 9 and 10, respectively, denote the results fitted by the constitutive models based on eight kinds of damage distribution, and the parameters of the fitted curves for various models are also presented in Figures 9 and 10. However, the slip zone soil of the Huangtupo landslide presents strain hardening characteristic under 400 kPa normal stress; therefore, the shear curve of the Huangtupo landslide under 400 kPa normal stress is not fitted, and only the shear deformation curves of 100 kPa, 200 kPa, 300 kPa normal stress were fitted. Test parameters K_s, u_y, and τ_r can be obtained from the ring shear tests, and the specific values are shown in Table 1.

Table 1. Parameters of ring shear test of the slip zone soil.

Slip Zone Soil	Normal Stress Level (kPa)	Shear Stiffness K_s (kPa/mm)	Shear Displacement at Yield Point u_y (mm)	Residual Strength τ_r (kPa)
A: Huangtupo landslide	100	165.390	0.294	45.853
	200	154.600	0.303	67.689
	300	174.210	0.314	97.356
	400	188.820	0.328	141.195
B: Shizibao landslide	200	152.320	0.563	76.693
	300	194.100	0.642	96.694
	400	200.900	0.651	131.752
	500	222.490	0.662	163.699

To measure the applicability of various constitutive models based on different damage distributions for different types of curves, the correlation coefficient R^2 was invited to evaluate the model quality and can be formulated as follows:

$$R^2 = 1 - \frac{\sum_{i=1}^{n} (\tau_i - \tau_{mi})^2}{\sum_{i=1}^{n} (\tau_i - \overline{\tau})^2} \tag{23}$$

where τ_i is the measured data of shear test, τ_{mi} is the fitting value of the model, $\overline{\tau}$ is the average value of the measured data, and n is the number of data obtained from the test. Figure 11 shows the correlation coefficient of each constitutive model, the average value of the correlation coefficient under different normal stresses, and the standard deviation.

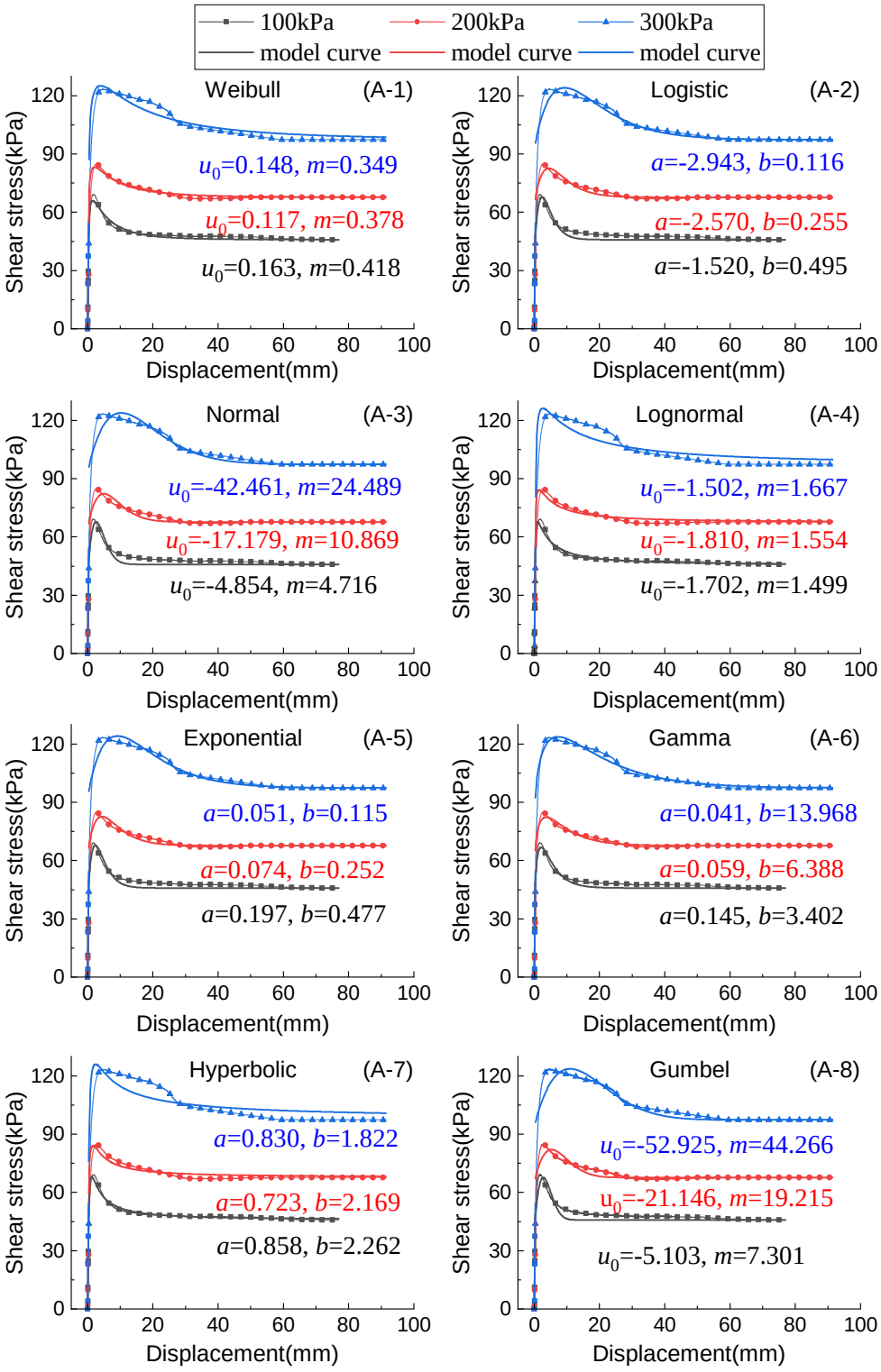

Figure 9. Fitting results of eight constitutive models on weaking softening type of shear curves. Series A presents the model curves and experimental data of the slip zone soil from Huangtupo landslide representing weak softening type. (**A-1**) Weibull-constitutive model; (**A-2**) logistic-constitutive model; (**A-3**) normal-constitutive model; (**A-4**) lognormal-constitutive model; (**A-5**) exponential-constitutive model; (**A-6**) Gamma-constitutive model; (**A-7**) hyperbolic-constitutive model; (**A-8**) Gumbel-constitutive model.

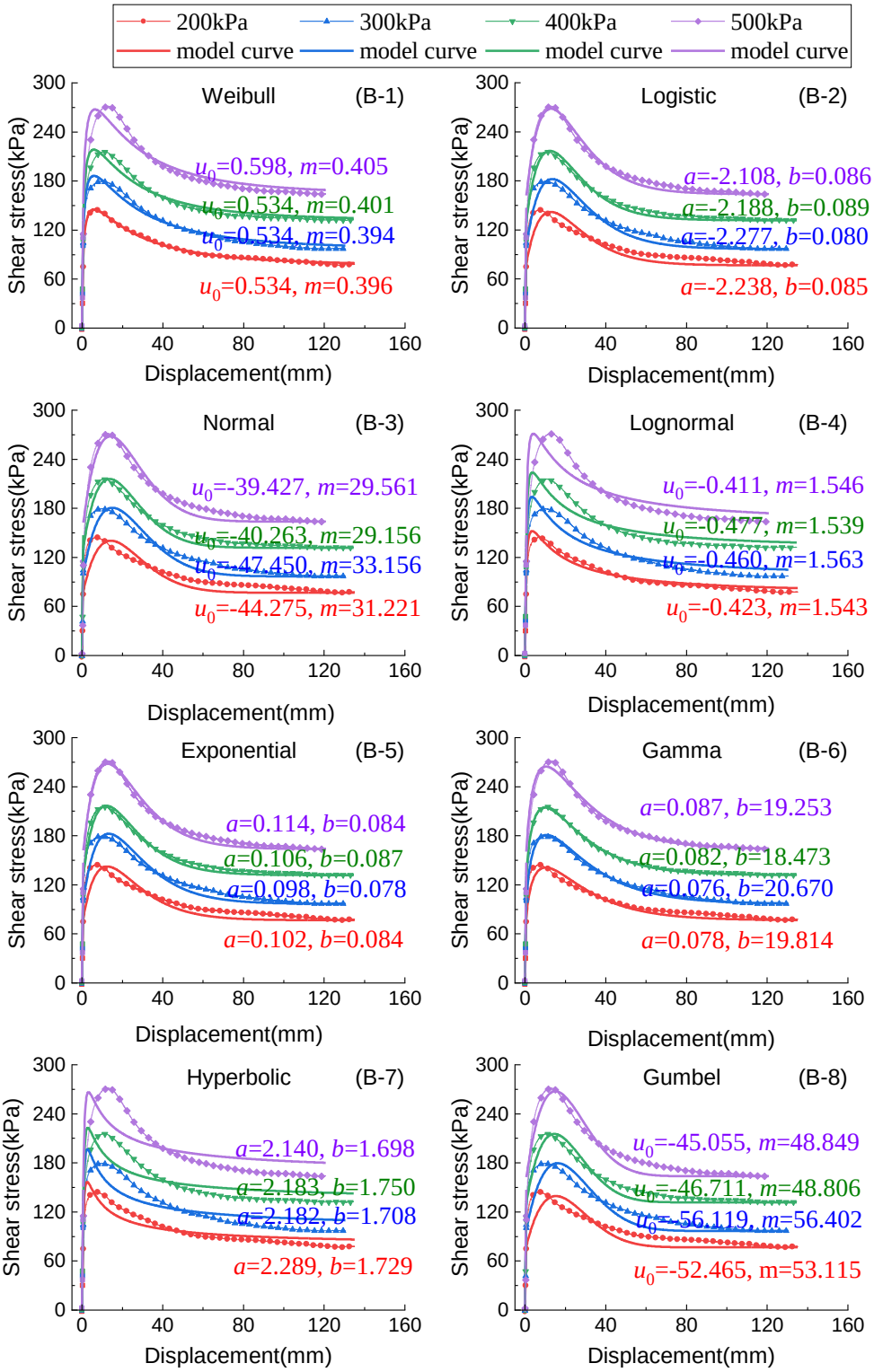

Figure 10. Fitting results of eight constitutive models on strong softening type of shear curves. Series B presents the model curves and experimental data of the slip zone soil from Shizibao landslide representing the strong softening type. (**B-1**) Weibull-constitutive model; (**B-2**) logistic-constitutive model; (**B-3**) normal-constitutive model; (**B-4**) lognormal-constitutive model; (**B-5**) exponential-constitutive model; (**B-6**) Gamma-constitutive model; (**B-7**) hyperbolic-constitutive model; (**B-8**) Gumbel-constitutive model.

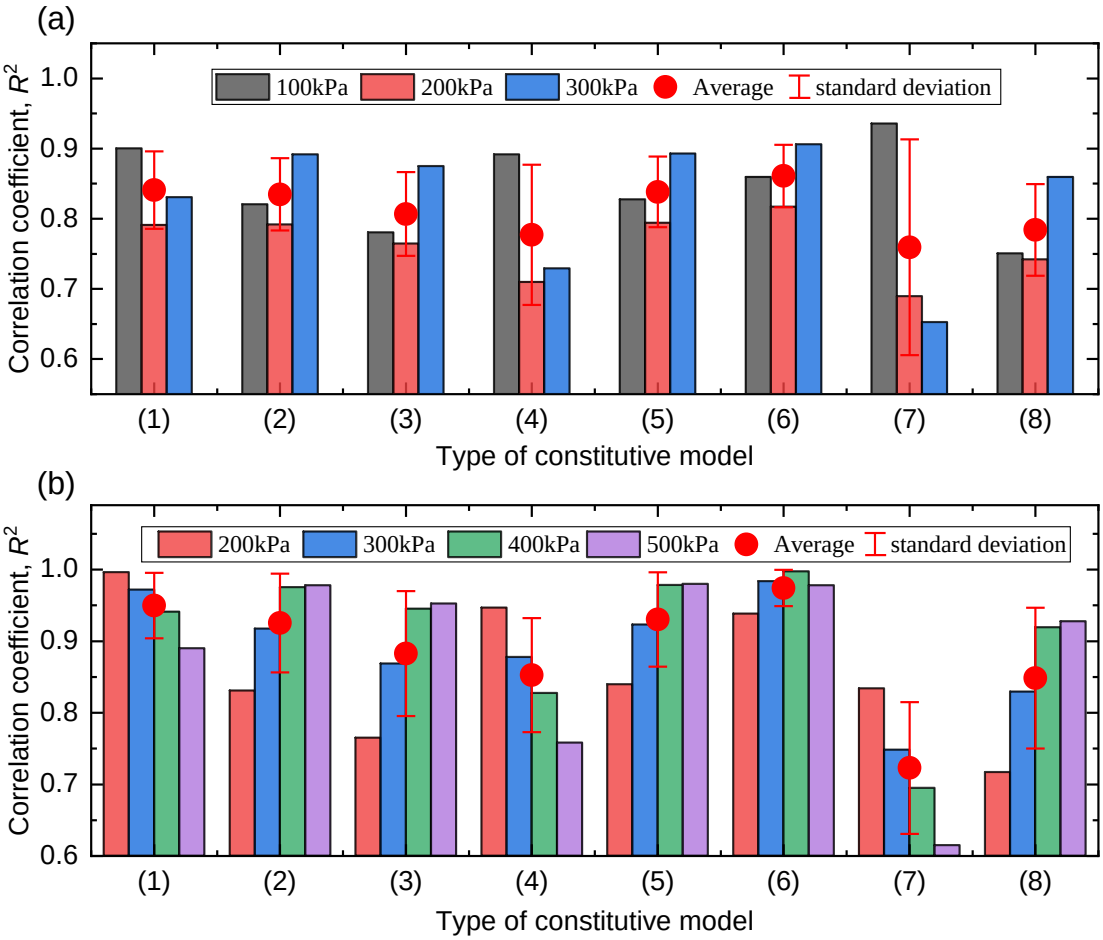

Figure 11. Correlation coefficient analysis of shear constitutive models. (**a**,**b**) Present the correlation coefficients of various shear constitutive models based on different distribution functions for Huangtupo landslide slip zone soil representing weak softening type, and for Shizibao landslide slip zone soil representing strong softening type, respectively. (1) Weibull-constitutive model; (2) logistic-constitutive model; (3) normal-constitutive model; (4) lognormal-constitutive model; (5) exponential-constitutive model; (6) Gamma-constitutive model; (7) hyperbolic-constitutive model; (8) Gumbel-constitutive model.

Combined with the fitting results and correlation analysis of each model, the test results were analyzed as follows:

(1) In the shear constitutive model based on Weibull distribution (Simplified as Weibull-constitutive model, and other models below were similar), the peak displacement of the model curve under high normal stress (400 kPa, 500kPa) in type B deviated to the left compared with the test data (Figure 10(B-1)). It showed better fitting results for type B test data under low normal stress and types A test data (Figure 9(A-1)). As a whole, the scale parameter u_0 of Weibull decreased with the increase of softening degree, and the shape parameter m increases with the increase of softening degree;

(2) The fitting correlation coefficients (R^2) of Logistic-constitutive model for type A curves were 0.821, 0.792, and 0.892 (Figure 11a). For type B curves, the fitting correlation coefficient increased from 0.831 to 0.978 as the normal stress increased (Figure 11b), which is better than that of type A curves. Parameter a increased with the increase of softening degree, but the influence of softening degree on parameter b was not clear;

(3) In the fitting result of the Normal-constitutive model, the peak displacement of model curves of type A in various normal stress and type B under low normal stress was greater than that of test data (Figure 9(A-3) and Figure 10(B-3)). The fitting result of

type B curve was better under high normal stress (400kPa, 500kPa), with correlation coefficients of 0.945 and 0.952 (Figure 11b);

(4) The fitting result of the Lognormal-constitutive model (Figure 10(B-4)) for type B curves shows that the peak displacement of simulated curves deviated to the left and the peak stress were higher compared with the test data. In general, the fitting results for type A (Figure 9(A-4)) were better than those for type B (Figure 10(B-4));

(5) The fitting result of the Exponential-constitutive model (Figures 9(A-5) and 10(B-5)) was similar to that of the Normal distribution, but the average fitting correlation coefficients of the two types of curves (R^2 were 0.838 and 0.930, respectively in Figure 11) were higher than those of the Normal-constitutive model (R^2 are 0.807 and 0.883, respectively in Figure 11). Parameters a and b decreased with the decrease of softening degree;

(6) The average fitting correlation coefficients (R^2) of the Gamma-constitutive model for type A and type B curves were 0.861 and 0.974, respectively (Figure 11), which were the highest among the eight models, and the standard error was small. It indicates that Gamma-constitutive model was the best choice for describing both two types of shear curves of the slip zone soil among the introduced models;

(7) Among the Hyperbolic-constitutive model, the fitting result of type A under normal stress 100 kPa was better, and the correlation coefficient was 0.936 (Figure 11a), but the characteristics of the model curves for type A under high normal stress and the model curves for type B (Figures 9(A-7) and 10(B-7)) were similar to the Lognormal-constitutive model;

(8) The fitting result of Gumbel-constitutive model shows that the peak displacement of the model for type B was greater than the actual peak displacement (Figure 10(B-8)). The fitting correlation coefficient increases from 0.717 to 0.928 as the normal stress increased (Figure 11b). The peak displacement of model curves for type A was also larger than the actual peak displacement (Figure 9(A-8)), but the peak displacement offset increased with the increase of normal stress.

The type A curves are the weak softening curves with the weak softening degree and even show hardening characteristics under the normal stress of 400kPa. It can be seen from Figure 11a, the applicability of various constitutive models for weak softening curves. The average of the correlation coefficients (R^2) of Lognormal, Hyperbolic, and Gumbel-constitutive models were less than 0.8, and the average correlation coefficient of the other five models was more than 0.8. It indicates that most of the above distributions were suitable for describing the damage evolution of type A curves. The average correlation coefficient (R^2) of the Gamma-constitutive model was 0.8609, indicating that Gamma distribution was the optimum for describing the damage evolution of weak softening type curve; The following optimal functions are Weibull-constitutive model (R^2 = 0.8408) and Exponential-constitutive model (R^2 = 0.8382).

The type B curves are the strong softening curves with a large softening degree. The simulated curves of the Lognormal, Hyperbolic, and Weibull-constitutive models show that the peak displacement deviates to the left (Figure 10), which indicates that the damage degree of these distributions reached the peak damage degree faster than the actual state with the displacement. It means that these models are not suitable for strong softening curves. The fitting results of other constitutive models show that the peak displacement of these models deviates slightly to the right under low normal stress (200 kPa and 300 kPa). While the fitting results under high normal stress are better, the average correlation coefficients of these models were greater than 0.8 (Figure 11b), indicating that these distributions conformed to the damage evolution law of type B curves. The average correlation coefficient of Gamma-constitutive model was 0.9744, which was the optimal constitutive model. The following are Exponential-constitutive model and Logistic-constitutive model, and the average correlation coefficient was 0.9303 and 0.9253, respectively.

In sum, the Gamma-constitutive model was the optimal shear constitutive model in both the strong softening curve and the weak softening curve, indicating that Gamma distribution was the most suitable for describing the dynamic damage process of slip zone soil. In addition, Exponential distribution was also one of the best models, which is a special case of Gamma distribution. Therefore, the superiority of Gamma distribution over other models can also be proved from this point. However, the commonly used Weibull-constitutive model was not suitable for the strong softening curve because of the large peak offset; it is only suitable for weak softening curves but is not the optimal model. The peak displacement of the strong softening curve fitting in most models deviates to the left or right. The results show that the damage evolution process of the strong softening shear curve was relatively unique, and there were few applicable damage distribution models. On the contrary, the weak softening curve was applicable to many models, and the deviation of peak displacement was small.

5. Discussion

5.1. Factors Affecting Softening Degree

In view of the above results, the applicability of various models to the two types of shear curves is obviously different. For the curves with different softening degrees, the appropriate damage distribution should be selected to construct the shear constitutive model. However, the softening degree is affected by many factors. For the same kind of soil, it shows the characteristics of weak softening curve when the pre-consolidation pressure and shear rate are small; when the pre-consolidation pressure and shear rate are large, the softening degree will increase, and it shows the characteristics of strong softening curve [43]. It is shown that the softening degree of the same soil will change under different stress histories and shear rates; thus, the change should be considered in the selection of damage distribution function. Other influencing factors, including moisture content [44,45], matrix suction [46], and powder content [47], also affect the softening degree by changing the peak strength or residual strength and the corresponding displacement. Therefore, the shear constitutive model of slip zone soil based on statistical damage should fully consider the factors that affect the softening characteristics, such as the type of slip zone soil, deformation speed, stress history, and moisture content, to select the most suitable model to represent the damage evolution process of slip zone soil.

5.2. Model Parameter Analysis

The above results indicate that the constitutive model based on Gamma distribution is the optimal model in both weak softening and strong softening curves. Therefore, the influence and the physical meaning of two parameters a and b of Gamma distribution on shear curve are further analyzed as below.

Figure 12 shows the constitutive model parameters a and b from Gamma distribution. In type A curves (Figure 12a), parameter a decreases, and parameter b increases with the increase of normal stress. In type B curves (Figure 12b), parameter a increases with the increase of normal stress. The softening characteristics of the two types of shear curves are opposite; thus, the changing trend of the constitutive model parameters a is also opposite.

The evolution curves of the damage variable based on Gamma-constitutive model (in Figure 13) demonstrate that the damage evolution changes nonlinearly with shear displacement. When the displacement reaches 5 mm, the damage variable of type A is more than 95% (Figure 13a); when the displacement reaches 5mm, the damage variable of type B is more than 90%, and the damage degree is close to 95% when the displacement reaches to 10 mm (Figure 13b). It shows that the damage variable has reached a higher degree of damage when the shear displacement is small. The above analysis also reveals that the soil is easy to be damaged under small deformation.

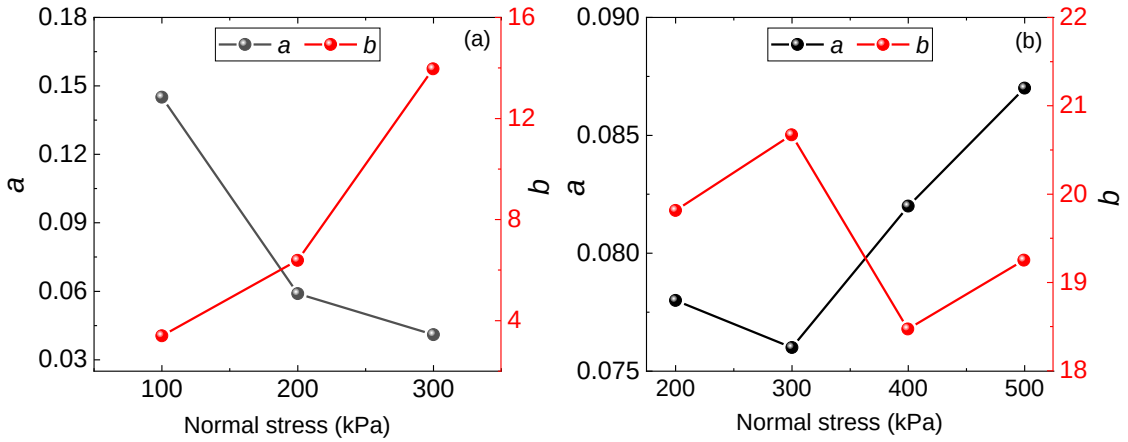

Figure 12. Parameters of the constitutive model based on Gamma distribution. (**a**) Gamma distribution parameter of type A curves; (**b**) Gamma distribution parameter of type B curves.

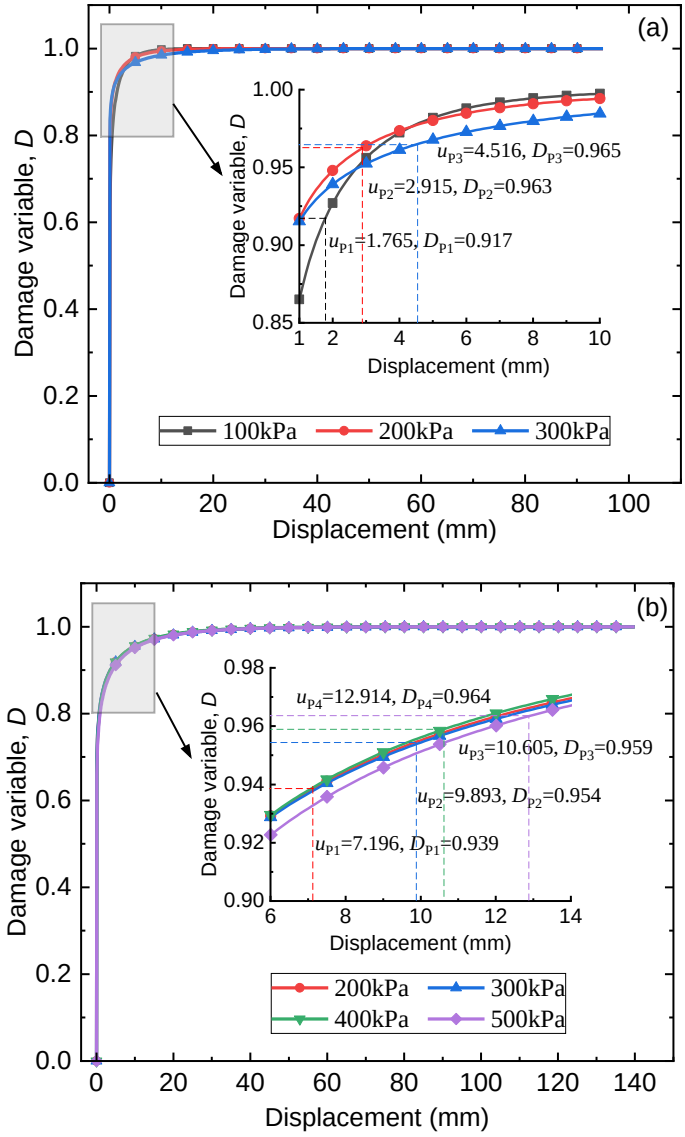

Figure 13. Evolution curves of damage variable based on Gamma distribution fitting results. (**a**) Damage evolution curves of type A; (**b**) damage evolution curves of type B.

The two parameters a and b of Gamma-constitutive model determine the shape of the shear softening curve and softening degree. Figure 14 shows how these two parameters affect the shape of the shear constitutive model curve by changing the values of parameters a or b and keeping other parameters constant. In Figure 14a, with the increase of parameter a, the peak stress and softening degree increase, but the peak displacement and the displacement reaching the residual strength also remain unchanged. It indicates that parameter a mainly determines the peak strength in the shear process. In Figure 14b, with the increase of parameter b, the peak strength and the corresponding peak displacement increase, and the displacement reaching the residual strength also increases. The increase of parameter b can also increase the softening degree and peak strength, but the influence on the strength is much less than parameter a. In sum, parameter a mainly determines the peak strength in shear deformation process, and the small increase of parameter a makes the peak value of shear constitutive model increase sharply; parameter b mainly determines the displacement reaching the peak strength and residual strength.

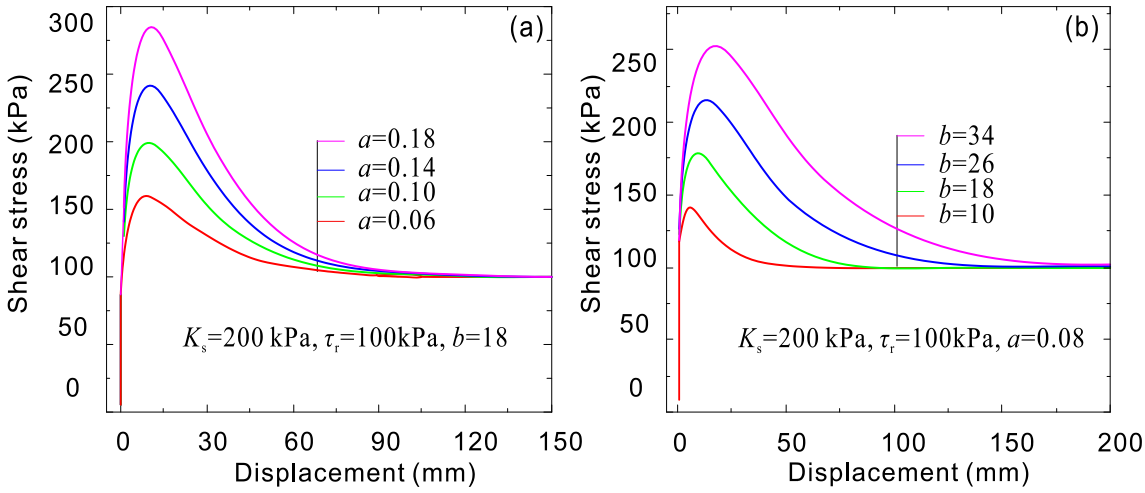

Figure 14. Effect of parameters of Gamma distribution on the shear curves. (**a**) model curves under various a values; (**b**) model curves under various b values.

6. Limitations and Future Works

Due to the lack of the sufficient number of ring shear test data, this paper cannot obtain a clear mechanism of softening influencing factors changing the damage evolution law of slip zone soil. In the future, more ring shear tests of slip zone soil need to be carried out to explore how the damage evolution changes and the internal relationship with the degree of softening.

7. Conclusions

This study investigated the relative merits of the eight damage statistical distributions in constructing the shear constitutive models of slip zone soil based on the statistical damage theory. In this paper, the fitting effects of constitutive models of eight damage distribution functions are analyzed, and the characteristics of constitutive models with different distribution functions are explored. The influencing factors of soil softening degree and the damage evolution characteristics in the process of soil shear are discussed. The main conclusions are as follows:

(1) The commonly used Weibull-constitutive model has a good fitting result in the weak softening curve, but it is not the optimal model. In the strong softening curve, the fitting result of the Weibull-constitutive model is poor, and the Weibull-constitutive model is not suitable for this kind of shear curve;

(2) The shear constitutive models based on Gamma distribution, Exponential distribution, and Logistic distribution are the best three models for the strong softening curve; the

shear constitutive models based on Gamma distribution, Weibull distribution, and Exponential distribution are the best three models for the weak softening curve. The results demonstrate that the Gamma distribution is the best distribution to reflect the damage evolution process of the slip zone soil;

(3) The physical meaning of the parameters in the constitutive model based on Gamma distribution is clear. Parameter *a* mainly determines peak strength and is a parameter reflecting strength; Parameter *b* determines the displacement of the peak strength and residual strength.

Author Contributions: Conceptualization, Z.Z. and Y.L.; data curation, C.L. and N.M.M.T.; methodology, Y.L., Z.Z. and H.D.; resources, Z.Z.; writing—original draft, Y.L. and Z.Z.; writing—review and editing, B.Z., B.D. and J.Z. All authors have read and agreed to the published version of the manuscript.

Funding: This research was funded by the National Natural Science Foundation of China (Nos. 42077268, 42020104006, 42090055), the Chongqing Geological Disaster Prevention and Control Center of China (No. 20C0023), and the China Three Gorges Corporation (No. 2019073).

Institutional Review Board Statement: Not applicable.

Informed Consent Statement: Informed consent was obtained from all subjects involved in the study.

Data Availability Statement: Not applicable.

Acknowledgments: This work was supported by the National Natural Science Foundation of China (Nos. 42077268, 42020104006, 42090055), the Chongqing Geological Disaster Prevention and Control Center of China (No. 20C0023), and the China Three Gorges Corporation (No. 2019073).

Conflicts of Interest: The authors declare no conflict of interest.

References

1. Zhang, Y.G.; Chen, X.Q.; Liao, R.P.; Wan, J.L.; He, Z.Y.; Zhao, Z.X.; Zhang, Y.; Su, Z.Y. Research on displacement prediction of step-type landslide under the influence of various environmental factors based on intelligent WCA-ELM in the Three Gorges Reservoir area. *Nat. Hazards* **2021**, *107*, 1709–1729. [CrossRef]
2. Zhang, Y.G.; Tang, J.; Liao, R.P.; Zhang, M.F.; Zhang, Y.; Wang, X.M.; Su, Z.Y. Application of an enhanced BP neural network model with water cycle algorithm on landslide prediction. *Stoch. Environ. Res. Risk Assess.* **2021**, *35*, 1273–1291. [CrossRef]
3. Terzaghi, K. *The Stability of Slopes in Theoretical Soil Mechanics*; Wiley: New York, NY, USA, 1943; pp. 144–181.
4. Lo, K.Y. An approach to the problem of progressive failure. *Can. Geotech. J.* **1972**, *9*, 407–429. [CrossRef]
5. Fan, N.; Jiang, J.; Dong, Y.; Guo, L.; Song, L. Approach for evaluating instantaneous impact forces during submarine slide-pipeline interaction considering the inertial action. *Ocean. Eng.* **2022**, *245*, 110466. [CrossRef]
6. Fang, K.; An, P.; Tang, H.; Tu, J.; Jia, S.; Miao, M.; Dong, A. Application of a multi-smartphone measurement system in slope model tests. *Eng. Geol.* **2021**, *295*, 106424. [CrossRef]
7. Tang, H.; Zou, Z.; Xiong, C.; Wu, Y.; Hu, X.; Wang, L.; Lu, S.; Criss, R.E.; Li, C. An evolution model of large consequent bedding rockslides, with particular reference to the Jiweishan rockslide in Southwest China. *Eng. Geol.* **2015**, *186*, 17–27. [CrossRef]
8. Wang, J.; Schweizer, D.; Liu, Q.; Su, A.; Hu, X.; Blum, P. Three-dimensional landslide evolution model at the Yangtze River. *Eng. Geol.* **2021**, *292*, 106275. [CrossRef]
9. Bandis, S.C.; Lumsden, A.C.; Barton, N.R. Fundamentals of rock joint deformation. *Int. J. Rock. Mech. Min.* **1983**, *20*, 249–268. [CrossRef]
10. Saeb, S.; Amadei, B. Modelling rock joints under shear and normal loading. *Int. J. Rock Mech. Min. Sci. Geomech. Abstr.* **1992**, *29*, 267–278. [CrossRef]
11. Grasselli, G.; Egger, P. Constitutive law for the shear strength of rock joints based on three-dimensional surface parameters. *Int. J. Rock Mech. Min.* **2003**, *40*, 25–40. [CrossRef]
12. Chan, D.H.; Morgenstern, N.R. Analysis of progressive deformation of the Edmonton Convention Centre excavation. *Can. Geotech. J.* **1987**, *24*, 430–440. [CrossRef]
13. Tiande, M.; Chongwu, M.; Shengzhi, W. Evolution Model of Progressive Failure of Landslides. *J. Geotech. Geoenviron. Eng.* **1999**, *125*, 827–831. [CrossRef]
14. Liu, C.N. Progressive failure mechanism in one-dimensional stability analysis of shallow slope failures. *Landslides* **2009**, *6*, 129–137. [CrossRef]
15. Chen, Z.; Morgenstern, N.R.; Chan, D.H. Progressive failure of the Carsington Dam: A numerical study. *Can. Geotech. J.* **1992**, *29*, 971–988. [CrossRef]

16. Zou, Z.; Yan, J.; Tang, H.; Wang, S.; Xiong, C.; Hu, X. A shear constitutive model for describing the full process of the deformation and failure of slip zone soil. *Eng. Geol.* **2020**, *276*, 105766. [CrossRef]
17. Yan, J.; Zou, Z.; Guo, S.; Zhang, Q.; Hu, X.; Luo, T. Mechanical behavior and damage constitutive model of granodiorite in a deep buried tunnel. *Bull. Eng. Geol. Environ.* **2022**, *81*, 118. [CrossRef]
18. Yan, J.; Zou, Z.; Mu, R.; Hu, X.; Zhang, J.; Zhang, W.; Su, A.; Wang, J.; Luo, T. Evaluating the stability of Outang landslide in the Three Gorges Reservoir area considering the mechanical behavior with large deformation of the slip zone. *Nat. Hazards* **2022**, 1–25. [CrossRef]
19. Kachanov, L.M. Time of the rupture process under creep conditions, Izy Akad. *Nank SSR Otd Tech. Nauk* **1958**, *8*, 26–31.
20. Krajcinovic, D.; Silva, M.A.G. Statistical aspects of the continuous damage theory. *Int. J. Solids Struct.* **1982**, *18*, 551–562. [CrossRef]
21. Lemaitre, J. How to use damage mechanics. *Nucl. Eng. Des.* **1984**, *80*, 233–245. [CrossRef]
22. Cao, W.G.; Zhao, H.; Li, X.; Zhang, Y.J. Statistical damage model with strain softening and hardening for rocks under the influence of voids and volume changes. *Can. Geotech. J.* **2010**, *47*, 857–871. [CrossRef]
23. Li, X.; Cao, W.G.; Su, Y.H. A statistical damage constitutive model for softening behavior of rocks. *Eng. Geol.* **2012**, *143–144*, 1–17. [CrossRef]
24. Shen, P.; Tang, H.; Ning, Y.; Xia, D. A damage mechanics based on the constitutive model for strain-softening rocks. *Eng. Fract. Mech.* **2019**, *216*, 106521. [CrossRef]
25. Zhang, H.; Hu, X.L.; Wu, S.S. Damage evolution of soil-rock mixture based on Fourier series approximations method. *J. Zhejiang Univ. (Eng. Sci.)* **2019**, *53*, 1955–1965. [CrossRef]
26. Zhang, Q.H.; Liu, Q.B.; Wang, S.H.; Liu, H.L.; Shi, G.H. Progressive Failure of Blocky Rock System: Geometrical–Mechanical Identification and Rock-Bolt Support. *Rock Mech. Rock Eng.* **2022**, *55*, 1649–1662. [CrossRef]
27. Weibull, W. A Statistical Distribution Function of Wide Applicability. *J. Appl. Mech.* **1951**, *18*, 293–297. [CrossRef]
28. Weddfelt, K.; Saadati, M.; Larsson, P.L. On the load capacity and fracture mechanism of hard rocks at indentation loading. *Int. J. Rock Mech. Min. Sci.* **2017**, *100*, 170–176. [CrossRef]
29. Xie, S.; Lin, H.; Chen, Y.; Yong, R.; Xiong, W.; Du, S. A damage constitutive model for shear behavior of joints based on determination of the yield point. *Int. J. Rock Mech. Min. Sci.* **2020**, *128*, 104269. [CrossRef]
30. Bao, L.; Zhang, G.; Hu, X.; Wu, S.; Liu, X. Stage Division of Landslide Deformation and Prediction of Critical Sliding Based on Inverse Logistic Function. *Energies* **2021**, *14*, 1091. [CrossRef]
31. Liu, D.Q.; Wang, Z.; Zhang, X.Y. Characteristics of strain softening of rocks and its damage constitutive model. *Yantu Lixue/Rock Soil Mech.* **2017**, *38*, 2901–2908. [CrossRef]
32. Cao, W.G.; Li, X.; Zhao, H. Damage constitutive model for strain-softening rock based on normal distribution and its parameter determination. *J. Cent. South Univ. Technol.* **2007**, *14*, 719–724. [CrossRef]
33. Ten Brink, U.S.; Barkan, R.; Andrews, B.D.; Chaytor, J.D. Size distributions and failure initiation of submarine and subaerial landslides. *Earth Planet Sci. Lett.* **2009**, *287*, 31–42. [CrossRef]
34. Milledge, D.G.; Bellugi, D.; McKean, J.A.; Densmore, A.L.; Dietrich, W.E. A multidimensional stability model for predicting shallow landslide size and shape across landscapes. *J. Geophys. Res. Earth Surf.* **2014**, *119*, 2481–2504. [CrossRef] [PubMed]
35. Qiu, H.; Hu, S.; Yang, D.; He, Y.; Pei, Y.; Kamp, U. Comparing landslide size probability distribution at the landscape scale (Loess Plateau and the Qinba Mountains, Central China) using double Pareto and inverse gamma. *Bull. Eng. Geol. Environ.* **2021**, *80*, 1035–1046. [CrossRef]
36. Feng, J.; Zhang, J.B.; Zhu, A.N.; Bi, J.W. Soil macropore structure characterized by X-ray computed tomography. *Pedosphere* **2003**, *13*, 289–298.
37. Purkait, B. The use of grain-size distribution patterns to elucidate aeolian processes on a transverse dune of Thar Desert, India. *Earth Surf. Process. Landf.* **2010**, *35*, 525–530. [CrossRef]
38. Lee, J.H.; Kim, H.; Park, H.J.; Heo, J.H. Temporal prediction modeling for rainfall-induced shallow landslide hazards using extreme value distribution. *Landslides* **2021**, *18*, 321–338. [CrossRef]
39. Wang, S.; Xiang, W.; Cui, D.S.; Yang, J.; Huang, X. Study of residual strength of slide zone soil under different ring-shear tests. *Yantu Lixue/Rock Soil Mech.* **2012**, *33*, 2967–2972.
40. Li, C.; Fu, Z.; Wang, Y.; Tang, H.; Yan, J.; Gong, W.; Yao, W.; Criss, R.E. Susceptibility of reservoir-induced landslides and strategies for increasing the slope stability in the Three Gorges Reservoir Area: Zigui Basin as an example. *Eng. Geol.* **2019**, *261*, 105279. [CrossRef]
41. Li, C.; Criss, R.E.; Fu, Z.; Long, J.; Tan, Q. Evolution characteristics and displacement forecasting model of landslides with stair-step sliding surface along the Xiangxi River, three Gorges Reservoir region, China. *Eng. Geol.* **2021**, *283*, 105961. [CrossRef]
42. Tang, H.; Wasowski, J.; Juang, C.H. Geohazards in the three Gorges Reservoir Area, China—Lessons learned from decades of research. *Eng. Geol.* **2019**, *261*, 105267. [CrossRef]
43. Hong, Y.; Yu, G.; Wu, Y.; Zheng, X. Effect of cyclic loading on the residual strength of over-consolidated silty clay in a ring shear test. *Landslides* **2011**, *8*, 233–240. [CrossRef]
44. Bao, H.; Qi, Q.; Lan, H.; Yan, C.; Feng, L.; Xu, J.; Yin, P.; Peng, J. Sliding mechanical properties of fault gouge studied from ring shear test-based microscopic morphology characterization. *Eng. Geol.* **2020**, *279*, 105879. [CrossRef]
45. Chen, C.; Wu, L.; Perdjon, M.; Huang, X.; Peng, Y. The drying effect on xanthan gum biopolymer treated sandy soil shear strength. *Constr. Build. Mater.* **2019**, *197*, 271–279. [CrossRef]

46. Hoyos, L.R.; Velosa, C.L.; Puppala, A.J. Residual shear strength of unsaturated soils via suction-controlled ring shear testing. *Eng. Geol.* **2014**, *172*, 1–11. [CrossRef]
47. Liu, D.; Chen, X.P. Laboratory Test and Parameter Back Analysis of Residual Strength of Slip Zone Soils. *J. South China Univ. Technol. (Nat. Sci. Ed.)* **2014**, *42*, 81–87. [CrossRef]